THE ASTROPHYSICAL JOURNAL, 237:290–302, 1980 April 1

THE ULTRAVIOLET CONTINUA OF THE NUCLEI OF M31 AND M81

CHI-CHAO WU
Computer Sciences Corporation
S. M. FABER[1]
Lick Observatory, Board of Studies in Astronomy and Astrophysics, University of California, Santa Cruz
J. S. GALLAGHER AND M. PECK
University of Illinois Observatory, Urbana
AND
B. M. TINSLEY[1]
Yale University Observatory
Received 1979 August 31; accepted 1979 October 5

ABSTRACT

We report ultraviolet measurements of the central 2'.5 of M31 and M81 made with the *ANS* satellite. A library of standard-star observations is also included for comparison. In agreement with *OAO 2* results, we find that both galaxies exhibit a significant UV excess as compared to expectations for a pure, old metal-rich stellar population including just the main sequence and giant branch. Model calculations show that the excess UV light could be produced either by young stars or by commonly occurring hot stars in an old stellar population. At the present time, several lines of evidence slightly favor old stars. An ultraviolet excess of similar magnitude seems to be common to all early-type galaxies yet observed in the UV and thus may significantly affect the appearance of redshifted galaxies.

Subject headings: galaxies: individual — galaxies: nuclei — galaxies: stellar content — spectrophotometry — ultraviolet: general

I. INTRODUCTION

Ultraviolet observations are vital to our understanding of galaxies, because they allow us to study hot members of the stellar population, which in most early-type galaxies make only a negligible contribution to the visible and infrared energy distributions. In this paper we describe UV observations of the nuclear bulges of M31 and M81. Much information is already available on the stellar content of these objects from studies at optical and IR wavelengths (e.g., Spinrad and Taylor 1971; Faber 1972; Baldwin *et al.* 1973; O'Connel 1976; Cohen 1979). For example, we know with certainty that the major portion of the visible and IR flux arises from an old metal-rich stellar population with a main-sequence turnoff near 1 $M_\odot$ and a giant branch similar to the old-disk giant branch in the solar neighborhood (Tinsley and Gunn 1976).

In agreement with the findings of Code and Welch (1979), our new UV data clearly indicate that the UV continua of these galaxies are much brighter than expected from the main-sequence and giant-branch components of the old stellar population alone. We have investigated several models for the source of the excess UV flux by adding various types of hot stars to the expected population of cool stars. Possible UV contributors which we have considered include planetary nebulae, blue stragglers, a metal-poor horizontal branch, and young stars.

[1] Alfred P. Sloan Foundation Fellow.

Whatever the identity of the hot component, UV measurements of old stellar populations such as these are bound to have major astrophysical implications. They shed light on the poorly understood late stages of stellar evolution for 1 $M_\odot$ stars and provide a crucial comparison with metal-enrichment and star-formation scenarios in models of galaxy formation. Most importantly, they are essential to understanding the properties of highly redshifted elliptical and S0 galaxies, which in turn are important as probes of galaxy formation, cluster evolution, and the deceleration parameter for the universe as a whole.

II. OBSERVATIONS AND RESULTS

The observations were taken with the University of Groningen experiment on board the *Astronomical Netherlands Satellite* (*ANS*). The instrument consisted of a 0.2 m Cassegrain telescope, followed by a five-channel grating spectrophotometer (van Duinen *et al.* 1975). The response functions of the channels were nearly rectangular, with central wavelengths and widths (in parentheses) of 1549 Å (149 Å), 1799 Å (149 Å), 2200 Å (200 Å), 2493 Å (150 Å), and 3294 Å, (101 Å). The entrance aperture was 2'.5 × 2'.5 and the pointing accuracy was better than 0'.5

Bright stars were observed in the "pointing mode," in which the telescope was aimed at the star with the shutter closed for dark measurements and opened for stellar measurements. A typical observation contained three dark integrations alternated with two stellar

TABLE 1

ULTRAVIOLET OBSERVATIONS OF M31 AND M81

Parameters	1550 Å	1800 Å	2200 Å	2500 Å	3300 Å
M31-SKY (counts s^{-1})	2.01	1.60	2.60	1.30	21.35
σ ($\pm$ counts s^{-1})	$\pm$0.12	$\pm$0.08	$\pm$0.07	$\pm$0.06	$\pm$0.18
Flux[a]	11.93	11.28	13.74	13.64	139.16
m_λ, observed	11.21	11.27	11.05	11.06	8.54
$(m_\lambda)_0$, corrected for $E(B-V) = 0.11$	10.32	10.40	9.99	10.26	7.98
M81-SKY (counts s^{-1})	0.27	0.43	0.46	0.32	4.94
σ ($\pm$ counts s^{-1})	$\pm$0.05	$\pm$0.08	$\pm$0.03	$\pm$0.02	$\pm$0.08
Flux[a]	1.60	3.03	2.40	3.36	32.20
m_λ, observed	13.39	12.70	12.95	12.59	10.13
$(m_\lambda)_0$, corrected for $E(B-V) = 0.16$	12.09	11.44	11.41	11.42	9.31

[a] 10^{-14} ergs cm^{-2} s^{-1} $Å^{-1}$.

integrations, each DARK consisting of six 8 s samples and each STAR consisting of ten 1 s or 8 s samples. For faint objects, the "offset," or sky-chopping, mode was used. A typical offset observation contained six to ten STAR-SKY pairs, each STAR and SKY lasting an integral multiple of 16 s. Net count rates were corrected for nonlinearity effects and sensitivity changes of the instrument, which were small and well monitored (see also Appendix A).

For pointing-mode measurements, a small SKY-DARK correction was also applied. Using the brightness of 50 blank sky positions, Kester (1976) and de Boer and Koorneef (1975) derived the following values for SKY-DARK (in counts per second), starting with the 1550 Å channel: 0.30 $\pm$ 0.03, -0.34 ± 0.03, -0.18 ± 0.02, -0.29 ± 0.02, 0.81 $\pm$ 0.06. For four of the channels, the DARK was brighter than the SKY as a result of scattered light from the internal Cerenkov light source when the shutter was closed.

The final net count rates were converted into absolute fluxes using the laboratory calibration (Aalders *et al.* 1975; Wesselius *et al.* 1979), and magnitudes were defined such that $M_\lambda = 0.00$ corresponds to $F_\lambda = 3.64 \times 10^{-9}$ ergs cm^{-2} s^{-1} $Å^{-1}$ (Oke and Schild 1970). Further details of the observations and reduction procedures can be found in Wu, Gilra, and van Duinen (1980) and Wesselius *et al.* (1979).

The tables of standard intrinsic stellar colors and the procedures used to obtain them are presented in the appendices. Observations for M31 and M81 are summarized in Table 1. The angular extent of M31 is too large to use the offset mode. The pointing mode was therefore used, the sequence including three DARK and three OBJECT integrations, alternately spaced. Each DARK and OBJECT contained nine 8 s samples. The observation was made in the low background portion of the satellite orbit, and the average count rates were constant over the entire observation. Four separate observations were made of M81, all obtained in the offset mode, with sky positions 25′ from the nucleus.

The 2.′5 × 2.′5 aperture of *ANS* lies well within the nuclear bulge of M31, and there is no chance of contamination by OB stars in the spiral arms. In M81, dust arms lie within the aperture, but the stellar population is amorphous, with no bright supergiants visible on a blue photograph (see Sandage 1961). Thus, it seems likely that in both galaxies, the observations refer to the inner bulge population only.

To add longer wavelength data to the ultraviolet observations, V and $(B-V)$ were linearly interpolated to a circular aperture of area equal to that of the square *ANS* aperture (see Table 2 for sources). A correction was also applied to adjust for reddening along the line of sight. For M31, we adopted $E(B-V) = 0.11$ (McClure and Racine 1969) and corrected the ultraviolet data using the mean *ANS* extinction curve (van

TABLE 2

ADOPTED MAGNITUDES AND COLORS FOR M31 AND M81

	V	B	3300 Å	2500 Å	2200 Å	1800 Å	1550 Å
M31, $E(B-V) = 0.11$:							
Raw magnitude, m_λ	6.50[a]	7.53[a]	8.54	11.06	11.05	11.27	11.21
Reddening-corrected magnitude $(m_\lambda)_0$	6.17	7.09	7.97	10.26	9.99	10.40	10.32
Color $(m_\lambda - V)_0$	0.00	0.92	1.81	4.09	3.82	4.23	4.15
σ (m_λ)	0.02	0.03	0.01	0.05	0.03	0.05	0.06
M81, $E(B-V) = 0.16$:							
Raw magnitude, m_λ	8.19[b]	9.19[b]	10.13	12.59	12.95	12.70	13.39
Reddening-corrected magnitude $(m_\lambda)_0$	7.71	8.55	9.31	11.42	11.41	11.44	12.09
Color $(m_\lambda - V)_0$	0.00	0.84	1.60	3.71	3.70	3.73	4.38
σ (m_λ)	0.05	0.05	0.02	0.06	0.06	0.19	0.19

[a] V, $B-V$ from observation by de Vaucouleurs and de Vaucouleurs 1972, with $\log A = 1.43$ extrapolated to $\log A = 1.45$.

[b] V, $B-V$ from extrapolation of 138″ aperture measurement by Sandage, Becklin, and Neugebauer 1969.

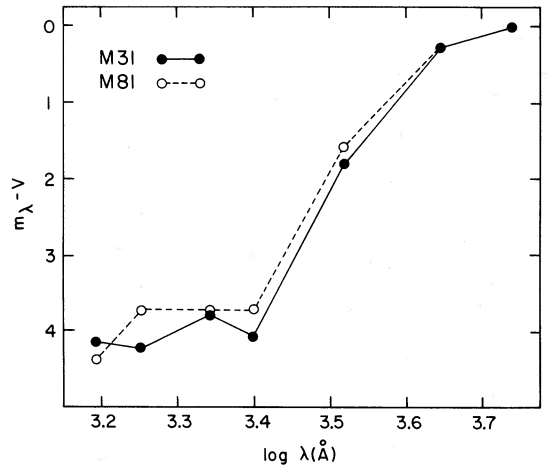

FIG. 1.—Reddening-corrected colors of M31 (*filled circles*) and M81 (*open circles*) from Table 2. (In this and the following figures, the *B* magnitude has been converted to an energy flux consistent with the calibration in Table 1.)

Duinen, Wu, and Kester 1976). For M81, the reddening is more difficult to estimate. The galactic reddening should be small, since the galactic latitude (41°) is fairly high. However, several dust lanes lie within the aperture, and the raw nuclear colors are several hundredths of a magnitude redder than those of M31, despite a similar mean metal abundance (cf. Spinrad and Taylor 1971). Both facts indicate that the reddening correction should therefore be higher than in M31; yet Peimbert (private communication to Spinrad and Taylor 1971) set an upper limit to the total reddening of 0.12 mag, based on the observed Balmer decrement in the nucleus. Here we adopt a total reddening of 0.16 mag, a value just sufficient to remove the absorption dip at 2200 Å, which is probably due to dust. However, this reddening value may be in error by as much as ± 0.05 mag.

The final adopted galaxy colors for both galaxies appear in Table 2 and Figure 1. The general level of UV flux is similar in both objects, but the exact shape is different. This could be important because, as is shown below, the detailed shape, in principle, carries significant clues to the identity of the hot component. However, the difference may stem in part from inexact reddening corrections. Since the correction for M81 is poorly determined, we confine ourselves to detailed population models for M31 only.

III. UNCONSTRAINED EMPIRICAL POPULATION MODELS

a) Procedure

To gain a general overview of the types of stars needed to match the flux distribution of M31, we have first computed unconstrained population models by combining the flux distribution of stars in various proportions that optimize the fit to the colors of M31. We initially experimented with both quadratic (Lasker 1970; Faber 1972) and linear (O'Connell 1976) algorithms, eventually choosing the latter for ease of computation (Peck 1980).

The system of equations solved was essentially identical to O'Connell's, except that our solutions contained no astrophysical constraints (cf. Turnrose 1976). The absolute values of the residuals in each filter were weighted inversely as the experimentally determined rms error in the galaxy observations at that wavelength.

Since the luminosity discrimination of our photometric system is poor, we confined our attention to determining the combination of temperatures needed to reproduce the M31 flux distribution. Unconstrained models were therefore computed based on a library of 60 main-sequence groups (O5 to M4). To this library we added the *ANS* data for the metal-poor globular cluster M13 (de Boer and van Albada 1976), for which we adopted $V = 6.87$ from Kron and Mayall (1960) and $E(B - V) = 0.02$ and $(B - V)_0 = 0.65$ from Burstein and McDonald (1975). A 50,000 K blackbody was also added to represent hot, compact objects such as planetary nuclei.

The energy distribution of M31 can be fitted by a synthetic stellar population with zero residuals in every passband and containing no more than seven nonzero stellar contributions. As there are only seven wavelengths observed, this is the maximum number of stellar groups needed to provide a basis vector which can reproduce the galaxy colors. Since such a solution has zero residuals, it is called "optimal." Optimal solutions are not unique, and in fact there are an infinite number of them. However, the space of optimal solutions is spanned by a large but finite number of basic solutions (no more than seven nonzero contributors), any linear combination of which is also an optimal formal solution to the problem. We have followed Peck (1980) in systematically exploring possible basic (or corner-point) solutions, a sample of which is given in Table 3.

A small number of suboptimal solutions were produced with random 1 σ perturbations of the galaxy colors to test the model's stability in the presence of photometric errors. No significant changes in the model temperature distribution resulted. The following conclusions based on these empirical models are also insensitive to the data longward of 3300 Å and do not depend on the photometric accuracy in any particular filter.

b) Discussion

All solutions (optimal and perturbed) contain four basic temperature groups:

1. Hot stars (O–early B) contribute ~98% of the flux at 1500 Å and ~1% at 3300 Å. Although the level of contribution is well determined and insensitive to photometric error or assumed foreground extinction, there is some ambiguity in the temperature distribution within this group. The hottest star in our library (a 50,000 K blackbody) may contribute as much as 40% at 1550 Å (model 1), with various combinations between this and an early–B-star–dominated model (models 6 and 7) allowable.

2. Intermediate temperature stars (A to early F) contribute 10–20% between 1800 and 2500 Å, but

TABLE 3

SAMPLE LINEAR-PROGRAMMING MODELS FOR M31 (PERCENTAGE LIGHT CONTRIBUTIONS)*

Wavelength, Å	1550	1800	2200	2500	3300	B	V
Stellar group			Model 1				
Black-body	40.38	28.20	10.14	8.44	.41	.05	.01
O7 V	58.14	49.71	23.36	17.40	.80	.10	.03
A5 V	1.03	17.82	14.15	13.39	2.58	1.57	.76
F8 V	.21	3.78	48.43	50.71	50.25	26.13	17.91
K0 V	.14	.35	3.52	8.91	40.00	46.35	41.50
K3 V	.00	.00	.00	.00	.01	.01	.01
M1 V	.10	.15	.40	1.15	5.96	25.79	39.77
Stellar group			Model 2				
O7 V	83.73	71.60	33.64	25.06	1.15	.15	.05
A5 V	.44	7.52	5.97	5.65	1.09	.66	.32
F8 V	.17	2.99	38.34	40.15	39.78	20.69	14.18
G2 V	.02	.17	2.84	3.71	6.87	4.07	3.06
K0 V	.15	.38	3.85	9.77	43.82	50.78	45.47
M4 V	.08	.12	.21	.81	3.98	18.69	33.09
M13	15.42	17.22	15.14	14.86	3.31	4.97	3.84
Stellar group			Model 3				
O7 V	84.14	71.94	33.80	25.18	1.15	.15	.05
A5 V	.45	7.70	6.11	5.78	1.11	.68	.33
F8 V	.15	2.73	35.05	36.70	36.37	18.91	12.96
G2 V	.04	.44	7.20	9.41	17.44	10.32	7.76
K1 V	.12	.26	2.40	6.30	29.88	39.39	38.59
K7 V	.10	.17	.70	2.16	10.82	25.73	38.58
M13	15.01	16.76	14.73	14.46	3.22	4.83	3.74
Stellar group			Model 4				
Black-body	23.87	16.67	6.00	4.99	.24	.03	.01
O7 V	74.80	63.96	30.05	22.38	1.02	.13	.04
A5 V	.91	15.63	12.41	11.74	2.26	1.37	.67
F8 V	.04	.66	8.52	8.92	8.84	4.60	3.15
F9 V	.17	2.69	40.65	44.98	52.60	27.10	19.10
K4 V	.20	.38	2.33	6.84	34.28	63.54	71.62
M2 V	.01	.02	.05	.15	.75	3.23	5.41
Stellar group			Model 5				
Black-body	35.99	25.13	9.04	7.52	.37	.04	.01
O7 V	62.60	53.53	25.15	18.73	.86	.11	.03
A5 V	.92	15.90	12.63	11.95	2.30	1.40	.68
F7 V	.20	4.11	38.50	39.57	33.53	17.12	11.41
F8 V	.04	.80	10.20	10.69	10.59	5.51	3.77
K0 V	.16	.41	4.18	10.59	47.52	55.06	49.30
M2 V	.08	.13	.30	.95	4.85	20.77	34.78
Stellar group			Model 6				
O7 V	8.80	7.52	3.53	2.63	.12	.02	.00
B1 V	90.15	77.80	37.58	30.13	1.51	.23	.08
A5 V	.61	10.55	8.38	7.93	1.52	.93	.45
F8 V	.20	3.63	46.49	48.68	48.23	25.08	17.19
K0 V	.13	.33	3.29	8.34	37.41	43.35	38.81
K5 V	.06	.10	.57	1.73	8.35	17.44	21.35
M3 V	.05	.08	.16	.57	2.86	12.96	22.11
Stellar group			Model 7				
O7 V	51.70	44.21	20.77	15.47	.71	.09	.03
B3 V	47.16	39.59	19.48	16.50	1.03	.22	.08
A5 V	.70	12.10	9.61	9.10	1.75	1.06	.52
F8 V	.20	3.60	46.11	48.28	47.84	24.87	17.05
K0 V	.13	.33	3.32	8.41	37.75	43.74	39.17
K5 V	.06	.10	.54	1.65	7.99	16.68	20.43
M3 V	.05	.08	.17	.59	2.94	13.32	22.73
Stellar group			Model 8				
Black-body	36.21	25.28	9.09	7.56	.37	.04	.01
O7 V	62.67	53.59	25.18	18.75	.86	.11	.03
A5 V	.45	7.81	6.20	5.87	1.13	.69	.33
F0 V	.25	9.78	16.53	15.93	5.47	3.01	1.67
F8 V	.17	3.01	38.54	40.36	39.99	20.79	14.25
K0 V	.16	.42	4.20	10.65	47.77	55.35	49.56
M3 V	.08	.12	.25	.88	4.42	20.01	34.14

*All models fit M31 with zero residuals.

are unimportant longward of 3300 Å ($\lesssim 5\%$) or in the far-UV. This group is subject to some variation due to photometric errors in the 1800 and 2200 Å filters and, even within the optimal solution space, interacts with the details of the hot-star and main-sequence components. On the other hand, no solution in which the intermediate temperature component disappears entirely has been found. We have also computed models in which M13 constitutes part or all of the intermediate temperature component (models 2 and 3).

3. A recurrent group near spectral type F8 (plus or minus one spectral subclass) is invariably found to be a substantial contributor to the blue and UV regions. We tentatively identify this group with the main-sequence turnoff. The location of the turnoff is very sensitive to the assumed reddening. A reddening of 0.09 mag leads to a turnoff at G4, for example.

4. A cool group with spectral types G–M clearly represents the giant branch, which dominates the light in the visible. Because our data extend only to the V band, the details of this group are the least well determined, with little discrimination between late G and early K stars and a completely indeterminate M star component.

It is encouraging that the main-sequence turnoff and cool giant component are in reasonable agreement with previous models (Pritchett 1977; O'Connell 1976; Faber 1972). Where allowed, earlier models have also included a hot star component in addition to the conventional cool population (O'Connell 1976; Joly 1974). The multiple-generation solution of O'Connell (1976) is quite similar to our own, with O–B stars contributing 0.1% and A to early F stars 0.9% at 5050 Å in his model.

IV. EVOLUTIONARY MODELS

The unconstrained synthesized models clearly indicate the need for several different ranges of stellar temperatures. We now use evolutionary models to ask how the required stellar mixture could have arisen from possible histories of star formation. Because of uncertainties in stellar evolution, this approach must be supplemented by trial-and-error additions of stellar types that might have been overlooked in the conventional evolutionary tracks.

a) A Conventional Old Population

As outlined in § I, optical and infrared data show that the center of M31 contains primarily metal-rich stars with a locus in the H-R diagram like the main sequence, subgiant, and giant branches of an old open cluster. Model populations of this type have often been synthesized to match the optical and infrared colors of elliptical galaxies, and here we have calculated UV colors for the elliptical galaxy models of Tinsley (1978). The proportions of stars of each type are provided by the models, and the stellar UV colors are given by the data for dwarfs and giants in Tables 5 and 6. Figure 2 shows the results for a population of age 10^{10} yr and metallicity $Z = 0.01$, chosen because its colors agree with M31 longward of 4000 Å. This model will be referred to as the conventional old population (COP) and used as a basis for later variants. It is clear from Figure 2 that the COP has far too little UV light. Since its bluest stars are at the early G turnoff, it lacks the intermediate and hot stars found necessary in the preceding analysis. Changes in the adopted age, reddening, or metallicity by factors of ~ 2 would alter the details, but would not resolve this large discrepancy.

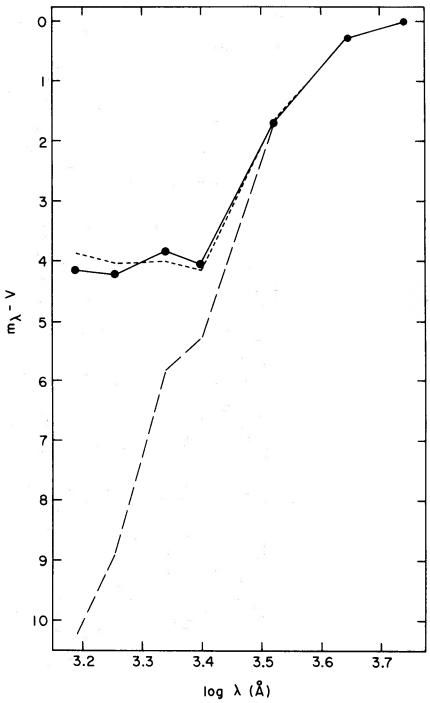

FIG. 2.—The UV flux distribution of M31 (*filled circles*) and two models obtained by evolutionary synthesis, using conventional stellar tracks in the H-R diagram plus the local IMF. *Long-dashed line*, for the "conventional old population" (COP) aged 10^{10} yr, containing only a main sequence up to an early G turnoff, corresponding subgiants, and a red-giant branch. Hotter stars are clearly needed to account for the data. *Short-dashed line*, best-fitting model with exponentially declining star formation; its time constant is 1.3×10^9 yr. Other models with ongoing or recent star formation provide no better fits, unless one allows a steeper IMF or several bursts of star formation.

The important question now is whether the hotter stars in M31 are simply normal members of an old population that were overlooked in constructing the COP, or young stars reflecting recent star formation near the galaxy's center.

b) Possible UV Sources in an Old Population

Hot stars in old stellar populations have been discussed previously by Hills (1971) and Tinsley (1971). Several types of hot stars might be included in realistic models for an old population, and we ask here whether they could account for the UV colors of M31.

Hot horizontal-branch stars and blue stragglers in a metal-rich population. Ciardullo and Demarque (1978) have suggested that blue horizontal-branch

stars arise from mass loss even in metal-rich old populations and contribute significantly to the blue light of elliptical galaxies. If this is the case, such stars would be important contributors in the UV. Exact predictions cannot be made, because the temperature distribution of these stars depends on poorly known details of stellar mass-loss rates. Nevertheless, Ciardullo and Demarque's results show qualitatively that the required hot and intermediate-temperature stars could plausibly be present in sufficient numbers.

This suggestion is apparently belied by the fairly metal-rich globular cluster 47 Tuc, which has only a red horizontal branch and is redder than M31 shortward of 2200 Å. Small-number statistics cannot be responsible for the spectral difference between M31 and 47 Tuc, since nearly 200 A0 horizontal-branch stars would be needed to give the same UV flux (relative to visual) as in M31. On the other hand, 47 Tuc might be a few billion years younger than most of the central stars in M31, in which case the higher turnoff mass would make a significant blue horizontal branch much less likely (Ciardullo and Demarque 1978).

The old metal-rich clusters NGC 188 and M67 contain blue stragglers, and M67 also has stars that could be members of a blue horizontal branch (Sargent 1968). Whatever their origin, these stars should be considered as possible constituents of normal nuclear-bulge populations. To model this possibility, we have computed the flux expected from the blue stragglers and horizontal-branch stars in M67, as given in Figure 4 of Racine (1971). This composite flux distribution has been added to the COP to give a best-fitting model using the linear-programming method (Fig. 3, *long-dashed line*). In the best model, 10% of the V light comes from the hot M67 component. The fit is good except at the shortest wavelengths, where it is seen that the bluest stars in M67 are not hot enough.

To rectify this problem, we next allowed the program to add any necessary hot stars from the stellar library to the preceding model (Fig. 3, *short-dashed line*). The fit is now greatly improved, although it is not exact at 1800 Å. The lack of an exactly fitting model based on the observed blue stars in M67 is not very significant, however, because the computed flux distribution is sensitive to the exact mixture of spectral types in the cluster, which is not well determined statistically because of the small numbers of stars involved.

We conclude that blue stragglers and/or horizontal-branch stars in an old metal-rich population could provide a satisfactory fit to the observed UV colors of M31.

Horizontal-branch stars in a minority metal-poor component. These stars should be considered, since there may be an appreciable mixture of metal abundances present in the inner bulge of M31. To model this possibility, M13 was used as the prototype of a metal-poor population. The linear-programming approach was used to constrain the contribution of M13 to be 50% at 2500 Å. (A higher percentage makes the 2500 color unacceptably blue.) The program

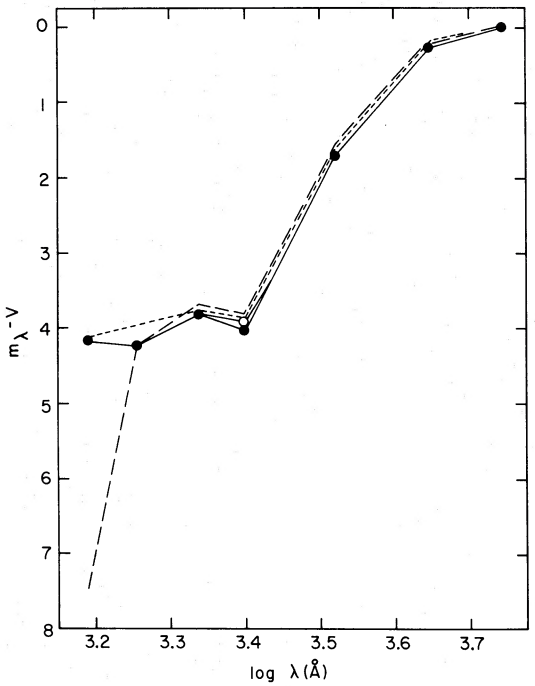

FIG. 3.—The UV flux distribution of M31 (*filled circles*) and three models containing hot stars that may belong to an old stellar population. *Long-dashed line*, best-fitting model with the COP (Fig. 2) and the composite flux distribution of the blue stragglers and horizontal branch stars in M67. *Short-dashed line*, preceding model optimized by the addition of hot stars from the stellar library. *Open circle* (other points coincide with the filled circles), refers to the best-fitting model in which the globular cluster M13 is constrained to produce 50% of the flux at 2500 Å (see Table 4).

was allowed to select from the stellar library to provide the additional necessary hotter and cooler components. The results are given in Table 4 and Figure 3 (*open circle*), where the fit is seen to be quite good.

In the model 5.7% of the V light arises from the metal-poor component. This percentage can be compared to the fraction of metal-poor clusters among the nuclear globulars in our own Galaxy. Harris's (1976) data on the distribution and metallicity of globular clusters in the Milky Way indicate that 4 out of 21 clusters (19%) having projected distances within 1 kpc of the galactic nucleus have spectral types of F5 or hotter and hence have hot horizontal branches. Searle and Zinn (1978) have also shown that globular clusters near the galactic center have a range in [Fe/H] from roughly -1.5 dex to solar, and metal-poor RR Lyrae stars (Butler, Carbon, and Kraft 1976) are also found in the bulge population. We conclude that the metal-poor population in proportion to that found in the nuclear bulge of our own Galaxy would be be more than adequate to produce the UV flux in M31.

It should be noted that the mean metallicity of globular clusters in M31 is $\sim$0.3 dex larger than that of the Milky Way globulars (cf. van den Bergh 1969), a fact which would tend to reduce the ultraviolet flux somewhat. However, a substantial UV contribution

still appears plausible owing to the very large spread in compositions which is probably present, if the nuclear bulge of our own Galaxy is any guide.

Nuclei of planetary nebulae. The hottest stars in our empirical model might plausibly be identified with the nuclei of planetary nebulae. Ford and Jacoby (1978) have surveyed the number of planetary nebulae within 3 mag of the brightest in the bulge of M31. Scaling their results to the *ANS* aperture, we find that detected planetaries (with $[M_{1550} - V]$ assumed to be -4 on the *ANS* system) contribute 10% of the flux in M31 at 1500 Å, thus falling short of the minimum requirements by a factor of 3 (see Table 4). In view of possible incompleteness in the survey plus possible contributions from planetaries below the magnitude limit, a shortfall of this size should perhaps be considered encouraging agreement. Indeed, the flux from nuclei of planetary nebulae that would be theoretically expected given the giant-branch visual luminosity is sufficient to account for the flux at 1550 Å (cf. Rose and Tinsley 1974).

Subdwarf O and B stars. The 1500 Å flux might also be emitted by subdwarf O and B stars of the type found in the galactic halo (Greenstein and Sargent 1974). These stars appear to be on the horizontal branch close to the helium-burning main sequence. Since the origin of these stars is unclear astrophysically, there is no good way to estimate their expected contribution relative to the cooler A type horizontal-branch stars.

White dwarfs. These cannot be the major intermediate-temperature component. For a white-dwarf cooling time of 3×10^9 yr (Lamb and Van Horn 1975) and M_v(WD) $- M_v$(K giant) ≈ 10, the contribution of white dwarfs is less than 10% of the required flux at 2500 Å.

Summarizing this section (§ IV*b*), we conclude that a suitable combination of blue stragglers, a metal-poor population, planetary nebulae, and hot subdwarfs could account for the UV continuum of M31.

c) Possibilities with Young Stars

Although no H II regions have been reported in the central region of M31 (Arp and Brueckel 1973), there is both dust (Johnson and Hanna 1972) and H I (Emerson 1974). The necessary raw materials for star formation are therefore present, and continuing or very recent star formation is a plausible source of early-type stars. Carruthers, Heckathorn, and Opal (1978) have suggested this possibility based on the elongated shape of the UV image of the nucleus.

We have computed a number of models incorporating a wide variety of star-formation histories. Exponentially declining rates of star formation, continuing star formation at constant rate but variable amplitude, and single bursts of variable age and amplitude have been investigated. The method of calculation and stellar evolutionary tracks are those used by Larson and Tinsley (1978). For simplicity, we used the initial mass function (IMF) of the solar neighborhood, as adopted in that paper. All luminosity classes in the stellar library have been used. The best-fitting exponential model is compared to M31 in Figure 2.

Briefly summarized, these experiments fail to match M31 very well, and the simple assumptions noted above must be relaxed if a better fit is desired. With continuing star-formation models, for example, one must adopt a steeper IMF, otherwise the hottest stars contribute too much light (e.g., Fig. 2). With the burst hypothesis, bursts of at least two ages and amplitudes are required in order to provide a large amount of A–F starlight plus a small amount of O–B starlight at the same time.

Although young star models, with these revisions, could provide a good match to the observations, they seem fundamentally at variance with the simple fact that no blue OB supergiants have been detected in the nuclear bulge of M31. NGC 205 provides a good comparison, for which the brightness at 1550 Å and 1800 Å is approximately 11.2 mag (de Boer, private communication). Approximately 47 stars between 19.4 and 21.0 B mag have been counted in NGC 205 within the *ANS* aperture (Hodge 1973), a number consistent with the observed UV flux. Since M31 is nearly 1 mag brighter than NGC 205 in the 1800 Å and 1550 Å filters, it ought to have roughly twice as many OB stars. The background light from the bulge in M31 is 17.5 to 18.0 B mag arcsec^{-2} (Light, Danielson, and Schwarzschild 1974) nearly 2 mag brighter than in NGC 205. This higher background would make such stars harder to detect. Nevertheless, van den Bergh (private communication) concludes from near-UV photographs that OB supergiants like those in NGC 205 are definitely not present in M31. Their absence would seem to argue in favor of hot objects

TABLE 4

MODEL FOR M31 WITH CONTRIBUTION FROM METAL-POOR GLOBULAR CLUSTERS CONSTRAINED TO BE 50% AT 2500 Å

Stellar Group	1550 Å	1800 Å	2200 Å	2500 Å	3300 Å	*B*	*V*
Blackbody	14.62	10.21	3.74	2.78	0.15	0.02	0.00
O5 V	28.57	24.43	11.69	7.79	0.39	0.04	0.01
F8 V	0.14	2.41	31.46	29.48	32.35	14.78	10.23
K1 V	0.09	0.21	1.94	4.56	23.95	27.75	26.02
K4 V	0.17	0.32	2.00	5.27	29.23	47.62	54.17
M1 V	0.01	0.02	0.04	0.11	0.65	2.49	3.87
M13	56.39	62.41	49.12	50.00	13.68	7.30	5.69
Model color	4.15	4.23	3.82	3.95	1.81	0.92	0.00
Galaxy color	4.15	4.23	3.82	4.09	1.81	0.92	0.00

of lower absolute magnitude of the sort expected in an aging stellar population. Code and Welch (1979) have reasoned along similar lines.

V. DISCUSSION

The ultraviolet flux distributions of M31 and M81 can be compared with *OAO* observations (Code and Welch 1979) of two normal luminous ellipticals and one S0. Although the *OAO* data do not extend to short wavelengths they generally resemble M31 down to the last measured point at 2500 Å. The UV flux level in the elliptical M32 is also similar to M31 (de Boer, private communication). Thus, there is moderately strong evidence in all these data that the UV excess in M31 is a universal phenomenon among old, spheroidal stellar populations. If true, this conclusion would be consistent with the idea that the UV excess is due to commonly occurring hot stars in an old population. The alternative hypothesis of young stars would imply that continuing star formation is a common property of E and S0 galaxies; this suggestion, at least for ellipticals, has recently been made as a possible interpretation of supernova statistics (Oemler and Tinsley 1979).

Accurate UV observations of early-type galaxies could conclusively determine whether their hot stars are mainly young or old. If due to young stars, the UV flux might vary widely from galaxy to galaxy as a function of the amplitude of ongoing star formation. We might also expect a strong radial decline in the UV continuum because bursts of star formation, when they do occur in early-type galaxies, are apparently highly concentrated to the nucleus (e.g., NGC 205 [Hodge 1973], NGC 5102 [Gallagher, Faber, and Balick 1975]). Conversely, a greater relative UV flux in ellipticals of low intrinsic luminosity or a radial increase away from the nucleus would argue strongly for contributions from a metal-poor component, since low-luminosity ellipticals and outer regions of galaxies tend to be relatively metal-poor. It would of course be important to select normal dust-free elliptical and S0 galaxies at high galactic latitude to minimize uncertainties due to reddening along the line of sight.

Code and Welch (1979) and Coleman, Wu, and Weedman (1980) have emphasized the fact that a UV excess in old stellar populations greatly affects the estimated *K*-corrections for distant early-type galaxies. If our flux distributions for M31 and M81 are at all typical of elliptical and S0 galaxies, *K*-corrections would certainly be much smaller than those estimated on the assumption of steep UV spectra. *K*-corrections based on M31, M81, Sc galaxies, and the Magellanic irregular NGC 4449 are being computed by Coleman, Wu, and Weedman (1980). Furthermore, the UV excesses may well have strong radial gradients, as mentioned above; so *K*-corrections will have corresponding gradients, and the luminosity profiles of distant galaxies will be altered. For example, if the UV excess is due to old stars and it increases radially outward because of a metallicity gradient, distant galaxies will appear more extended than their nearby counterparts. Both isophotal diameters and "metric" diameters derived from fitting surface-brightness profiles to an assumed function will be affected.

VI. SUMMARY

The central 2'.5 of M31 and M81 exhibit a significant ultraviolet excess as compared to expectations for a pure old metal-rich stellar population including just the main sequence and giant branch. Our measurements are in qualitative agreement with the results from *OAO 2* (Code and Welch 1979), but we find a generally declining flux for $\lambda < 2500$ Å with no significant upturn at 1550 Å.

Empirical linear-programming models of the stellar population in M31 indicate that four separate temperature groups of stars are required. These include a hot component (O to early B), intermediate component (late B to early F), a main-sequence turnoff group near G0, and cool giants. Evolutionary models are constructed based on young stars and on expected types of hot stars in an old population. Several lines of evidence slightly favor old stars at this time. Additional UV observations could allow us to choose between these alternatives.

The UV excess in these two galaxies seems to be present in several other normal early-type galaxies observed by *OAO* and *ANS*. This excess may therefore be common to all old stellar populations. If true, this result will modify *K*-corrections and might significantly affect the appearance of redshifted galaxies.

We wish to thank the members of the University of Groningen *ANS* UV team, Drs. J. W. G. Aalders, K. S. de Boer, K. J. van Duinen, D. Kester, and P. R. Wesselius, for their help in obtaining the data. The *ANS* project was sponsored by the Dutch Committee for Geophysics and Space Research of the Netherlands Academy of Sciences. Mr. Allan Wirth helped with the population synthesis models. We thank Drs. Pierre Demarque and Ron Webbink for discussions about stellar evolution, and Sidney van den Bergh for his information concerning UV photographs of the nuclear region of M31. This work was supported in part by NASA grants 7259 and 7343. NSF grants AST 76-08258 and AST 77-23566, and the Alfred P. Sloan Foundation.

APPENDIX A

INTRINSIC STELLAR COLORS

This appendix presents the adopted intrinsic colors of normal stars which have been used in the population synthesis. The observed stellar magnitudes from § II were corrected for interstellar reddening using the average *ANS* reddening law (van Duinen, Wu, and Kester 1976). $E(B - V)$ was obtained from the intrinsic $B - V$

colors of FitzGerald (1970) for stars with spectral type G9 and earlier. For stars later than G9, the intrinsic $B - V$ colors of Schmidt-Kaler (1965) were used. The V magnitudes were corrected assuming $A_v = 3.1\ E(B - V)$. The de-reddened $(m_\lambda)_0$ and V_0 were then combined to give the $(m_\lambda - V)_0$ colors as presented in Tables 5, 6, and 7.

TABLE 5

ULTRAVIOLET INTRINSIC COLORS, $(m_\lambda - V)_0$, OF DWARFS AND SUBGIANTS

Sp Type (1)	$(B - V)_0$ (2)	Number of Stars (3)	1550 Å (4)	1800 Å (5)	2200 Å (6)	2500 Å (7)	3300 Å (8)
O3–O5	−0.32	4	−4.47 ± 0.16	−4.21 ± 0.12	−3.68 ± 0.16	−3.15 ± 0.09	−1.97 ± 0.06
O6	−0.32	2	−4.18 ± 0.02	−3.94 ± 0.02	−3.35 ± 0.01	−2.93 ± 0.04	−1.89 ± 0.01
O7	−0.32	1	−4.13	−3.88	−3.49	−2.92	−1.82
O8	−0.31	1	−3.98	−3.80	−3.49	−2.98	−1.86
O9	−0.31	2	−4.11 ± 0.03	−3.86 ± 0.02	−3.46 ± 0.03	−2.95 ± 0.00	−1.83 ± 0.00
O9.5	−0.30	1	−3.97	−3.71	−3.26	−2.81	−1.76
B0	−0.30	1	−4.03	−3.70	−3.25	−2.77	−1.71
B0.5	−0.28	2	−3.88 ± 0.02	−3.58 ± 0.00	−3.18 ± 0.07	−2.69 ± 0.01	−1.67 ± 0.01
B1	−0.26	1	−3.64	−3.40	−3.03	−2.54	−1.55
B1.5	−0.25	3	−3.57 ± 0.01	−3.32 ± 0.01	−2.88 ± 0.02	−2.46 ± 0.01	−1.52 ± 0.01
B2	−0.24	8	−3.30 ± 0.04	−3.05 ± 0.03	−2.69 ± 0.03	−2.25 ± 0.03	−1.37 ± 0.02
B2.5	−0.22	6	−3.07 ± 0.06	−2.82 ± 0.06	−2.46 ± 0.06	−2.05 ± 0.06	−1.23 ± 0.04
B3 V	−0.20	15	−2.93 ± 0.02	−2.66 ± 0.02	−2.32 ± 0.02	−1.89 ± 0.02	−1.13 ± 0.01
B3 IV	−0.20	7	−2.83 ± 0.04	−2.61 ± 0.04	−2.25 ± 0.03	−1.85 ± 0.03	−1.11 ± 0.02
B4	−0.18	6	−2.76 ± 0.06	−2.52 ± 0.05	−2.14 ± 0.04	−1.78 ± 0.04	−1.08 ± 0.03
B5	−0.16	7	−2.48 ± 0.02	−2.24 ± 0.02	−1.89 ± 0.02	−1.54 ± 0.02	−0.93 ± 0.01
B6	−0.14	6	−2.29 ± 0.04	−2.06 ± 0.04	−1.74 ± 0.04	−1.39 ± 0.03	−0.84 ± 0.03
B7	−0.13	4	−1.96 ± 0.12	−1.76 ± 0.11	−1.49 ± 0.08	−1.13 ± 0.08	−0.64 ± 0.07
B8	−0.11	5	−1.56 ± 0.07	−1.40 ± 0.07	−1.14 ± 0.05	−0.81 ± 0.06	−0.42 ± 0.05
B9	−0.07	3	−1.03 ± 0.08	−0.96 ± 0.05	−0.74 ± 0.07	−0.43 ± 0.05	−0.15 ± 0.03
B9.5	−0.04	3	−1.00 ± 0.08	−0.93 ± 0.05	−0.73 ± 0.01	−0.40 ± 0.04	−0.15 ± 0.02
A0	−0.01	9	−0.39 ± 0.07	−0.51 ± 0.05	−0.34 ± 0.04	−0.05 ± 0.04	+0.09 ± 0.02
A1	+0.02	4	+0.07 ± 0.11	−0.25 ± 0.04	−0.07 ± 0.03	+0.19 ± 0.03	+0.19 ± 0.02
A2	+0.05	4	+0.85 ± 0.04	−0.01 ± 0.02	+0.10 ± 0.04	+0.37 ± 0.04	+0.24 ± 0.01
A3	+0.08	4	+1.68 ± 0.21	+0.28 ± 0.06	+0.29 ± 0.04	+0.59 ± 0.06	+0.34 ± 0.03
A4	+0.12	2	+2.87 ± 0.19	+0.53 ± 0.06	+0.49 ± 0.04	+0.74 ± 0.04	+0.39 ± 0.02
A5	+0.15	4	+3.70 ± 0.47	+0.69 ± 0.03	+0.51 ± 0.06	+0.82 ± 0.04	+0.36 ± 0.05
A6	+0.18	1	+4.17	+0.95	+0.78	+1.04	+0.43
A7	+0.20	3	+4.56 ± 0.16	+1.09 ± 0.10	+0.81 ± 0.09	+1.09 ± 0.08	+0.48 ± 0.06
A8	+0.27	2	+5.87 ± 0.04	+1.49 ± 0.12	+1.01 ± 0.02	+1.28 ± 0.00	+0.43 ± 0.01
A9	+0.30	1	+6.08	+2.01	+1.35	+1.58	+0.51
F0	+0.32	3	+6.08 ± 0.15	+2.19 ± 0.05	+1.19 ± 0.12	+1.48 ± 0.10	+0.39 ± 0.07
F1	+0.34	...	+6.24	+2.31	+1.25	+1.53	+0.39
F2	+0.35	...	+6.40	+2.42	+1.30	+1.58	+0.40
F3	+0.41	...	+6.84	+2.88	+1.48	+1.74	+0.44
F4	+0.42	...	+7.24	+3.34	+1.68	+1.94	+0.46
F5	+0.45	...	+7.68	+3.88	+1.88	+2.14	+0.47
F6	+0.48	...	+8.10	+4.50	+2.12	+2.36	+0.49
F7	+0.50	...	+8.44	+5.22	+2.36	+2.58	+0.51
F8	+0.53	...	+8.84	+5.80	+2.60	+2.80	+0.56
F9	+0.56	...	+9.16	+6.24	+2.86	+3.00	+0.58
G0	+0.60	...	+9.38	+6.62	+3.18	+3.22	+0.64
G1	+0.62	...	+9.56	+6.94	+3.46	+3.46	+0.74
G2	+0.63	...	+9.70	+7.22	+3.76	+3.72	+0.80
G3	+0.65	...	+9.80	+7.54	+4.14	+3.93	+0.90
G4	+0.66	...	+9.88	+7.82	+4.50	+4.16	+1.02
G5	+0.68	...	+9.96	+8.10	+4.86	+4.40	+1.17
G6	+0.72	...	+10.04	+8.36	+5.20	+4.61	+1.28
G7	+0.73	...	+10.08	+8.62	+5.50	+4.85	+1.38
G8	+0.74	...	+10.14	+8.88	+5.80	+5.10	+1.48
G9	+0.76	...	+10.20	+9.06	+6.10	+5.32	+1.60
K0	+0.81	...	+10.24	+9.30	+6.36	+5.60	+1.72
K1	+0.85	...	+10.28	+9.48	+6.64	+5.84	+1.90
K2	+0.89	...	+10.32*	+9.60*	+6.90*	+6.06*	+2.08*
K3	+0.97	...	+10.36*	+9.70*	+7.18*	+6.27*	+2.28*
K4	+1.06	...	+10.40*	+9.80*	+7.40*	+6.48	+2.48*
K5	+1.15	...	+10.44*	+9.90*	+7.62*	+6.66*	+2.70*
K6	+1.26	...	+10.48*	+10.00*	+7.82*	+6.88*	+2.89*
K7	+1.37	...	+10.52*	+10.03*	+8.04*	+7.06*	+3.06*
K8	+1.38	...	+10.54*	+10.06*	+8.22*	+7.24*	+3.24*
K9	+1.39	...	+10.54*	+10.10*	+8.40*	+7.42*	+3.42*
M0	+1.40	...	+10.56*	+10.13*	+8.56*	+7.58*	+3.58*
M1	+1.47	...	+10.56*	+10.16*	+8.68*	+7.78*	+3.74*
M2	+1.49	...	+10.58*	+10.20*	+8.84*	+7.84*	+3.82*
M3	+1.51	...	+10.60*	+10.24*	+9.00*	+7.90*	+3.90*
M4	+1.55	...	+10.62*	+10.24*	+9.16*	+7.96*	+3.98*

TABLE 6

ULTRAVIOLET INTRINSIC COLORS, $(m_\lambda - V)_0$, OF GIANTS AND BRIGHT GIANTS

Sp Type (1)	$(B-V)_0$ (2)	Number of Stars (3)	1550 Å (4)	1800 Å (5)	2200 Å (6)	2500 Å (7)	3300 Å (8)
B0	−0.30	4	−3.91 ± 0.01	−3.69 ± 0.01	−3.38 ± 0.03	−2.85 ± 0.02	−1.78 ± 0.01
B0.5	−0.28	1	−3.65	−3.47	−3.18	−2.72	−1.71
B1	−0.26	2	−3.63 ± 0.04	−3.39 ± 0.04	−2.99 ± 0.02	−2.55 ± 0.01	−1.59 ± 0.01
B1.5	−0.25	4	−3.25 ± 0.05	−3.07 ± 0.04	−2.83 ± 0.03	−2.39 ± 0.03	−1.47 ± 0.02
B2	−0.24	6	−3.18 ± 0.11	−2.98 ± 0.09	−2.67 ± 0.05	−2.26 ± 0.05	−1.40 ± 0.03
B2.5	−0.22	3	−2.89 ± 0.08	−2.71 ± 0.05	−2.43 ± 0.04	−2.02 ± 0.01	−1.25 ± 0.03
B3	−0.20	1	−2.76	−2.55	−2.23	−1.82	−1.12
B4	−0.18	3	−2.58 ± 0.03	−2.36 ± 0.02	−2.01 ± 0.06	−1.64 ± 0.03	−1.00 ± 0.01
B5	−0.16	6	−2.28 ± 0.06	−2.09 ± 0.06	−1.78 ± 0.06	−1.45 ± 0.05	−0.91 + 0.04
B6	−0.14	2	−2.24 ± 0.11	−1.99 ± 0.10	−1.67 ± 0.10	−1.31 ± 0.08	−0.79 + 0.05
B7	−0.12	2	−1.81 ± 0.03	−1.64 ± 0.07	−1.31 ± 0.10	−1.02 ± 0.08	−0.65 ± 0.04
B8	−0.10	4	−1.64 ± 0.08	−1.47 ± 0.07	−1.21 ± 0.07	−0.87 ± 0.06	−0.52 ± 0.06
B9	−0.08	3	−0.87 ± 0.12	−0.82 ± 0.11	−0.66 ± 0.11	−0.30 ± 0.09	−0.11 ± 0.01
B9.5	−0.05	3	−0.67 ± 0.07	−0.65 ± 0.05	−0.46 ± 0.06	−0.16 ± 0.05	+0.01 ± 0.06
A0	−0.03	3	−0.25 ± 0.06	−0.40 ± 0.04	−0.25 ± 0.04	+0.06 ± 0.04	+0.13 ± 0.05
A1	+0.01	0	+0.42	−0.10	−0.01	+0.29	+0.23
A2	+0.05	0	+1.09	+0.19	+0.23	+0.51	+0.34
A3	+0.09	2	+1.76 ± 0.02	+0.49 ± 0.04	+0.47 ± 0.05	+0.74 ± 0.01	+0.44 ± 0.00
A4	+0.12	0	+2.63	+0.69	+0.62	+0.86	+0.48
A5 III	+0.15	1	+3.49	+0.88	+0.77	+0.98	+0.51
A5 II	+0.10	1	+2.94	+1.36	+1.28	+1.40	+0.84
A6	+0.20	0	+4.15	+1.18	+0.96	+1.18	+0.56
A7	+0.24	0	+4.81	+1.49	+1.15	+1.38	+0.60
A8	+0.26	0	+5.46	+1.79	+1.34	+1.58	+0.65
A9	+0.28	1	+6.12	+2.09	+1.53	+1.78	+0.69
F0	+0.32	1	(+7.17)	+2.67	+1.77	+1.93	+0.74
F1	+0.33	...	+6.25	+2.79	+1.92	+2.04	+0.80
F2	+0.36	...	+6.32	+2.90	+2.06	+2.14	+0.86
F3	+0.39	...	+6.70	+3.26	+2.26	+2.30	+0.90
F4	+0.42	...	+7.02	+3.66	+2.48	+2.46	+0.94
F5	+0.43	...	+7.32	+4.02	+2.70	+2.62	+0.98
F6	+0.46	...	+7.60	+4.40	+2.90	+2.78	+1.06
F7	+0.48	...	+7.88	+4.76	+3.08	+2.94	+1.12
F8	+0.52	...	+8.12	+5.10	+3.30	+3.12	+1.20
F9	...	...	+8.36	+5.42	+3.52	+3.28	+1.24
G0	+0.64	...	+8.62	+5.74	+3.76	+3.46	+1.30
G1	+0.69	...	+8.88	+6.08	+4.02	+3.62	+1.34
G2	+0.77	...	+9.08	+6.42	+4.30	+3.82	+1.37
G3	+0.85	...	+9.30	+6.80	+4.64	+4.04	+1.40
G4	+0.88	...	+9.52	+7.16	+5.02	+4.34	+1.45
G5	+0.90	...	+9.74	+7.68	+5.46	+4.70	+1.50
G6	+0.92	...	+9.92	+8.30	+5.98	+5.08	+1.57
G7	+0.94	...	+10.06	+9.00	+6.56	+5.48	+1.64
G8	+0.95	...	+10.20	+9.56	+7.10	+5.84	+1.78
G9	+0.98	...	+10.34	+9.88	+7.56	+6.20	+1.95
K0	+0.99	...	+10.46	+10.06	+7.96	+6.56	+2.02
K1	+1.07	...	+10.52	+10.16	+8.26	+7.02	+2.18
K2	+1.16	...	+10.60	+10.22	+8.56	+7.42	+2.58
K3	+1.28	...	+10.64	+10.28	+8.84	+7.74	+3.12
K4	+1.39	...	+10.72	+10.34	+9.06	+8.02	+3.64
K5	+1.50	...	+10.76	+10.40	+9.24	+8.24	+4.06
K6	+1.52	...	+10.78	+10.42	+9.40	+8.40	+4.13
K7	+1.53	...	+10.80	+10.42	+9.50	+8.52	+4.30
K8	+1.53	...	+10.80	+10.42	+9.58	+8.64	+4.33
K9	+1.54	...	+10.80	+10.42	+9.68	+8.74	+4.38
M0	+1.54	...	+10.80	+10.42	+9.68	+8.76	+4.40
M1	+1.55	...	+10.80	+10.42	+9.70	+8.76	+4.40
M2	+1.57	...	+10.80	+10.42	+9.74	+8.78	+4.40
M3	+1.60	...	+10.80	+10.42	+9.78	+8.80	+4.40
M4	+1.68	...	+10.80*	+10.42*	+9.82*	+8.82*	+4.40*

Columns (1) and (2) contain the spectral type and intrinsic $B - V$. Column (3) indicates the number of stars combined to form the average. A zero in column (3) shows that no star was observed. In this case the intrinsic colors were obtained by graphical interpolation between neighboring subtypes (see below). Columns (4) through (8) contain the intrinsic colors. If two or more stars are available, the rms scatter in their intrinsic colors is also included. For early-type stars (F0 or hotter), the count rates were generally high. Since each individual star almost always has several observations, the internal error is usually two to three hundredths of a magnitude or smaller.

TABLE 7

ULTRAVIOLET INTRINSIC COLORS, $(m_\lambda - V)_0$, OF SUPERGIANTS

Sp Type (1)	$(B-V)_0$ (2)	Number of Stars (3)	1550 Å (4)	1800 Å (5)	2200 Å (6)	2500 Å (7)	3300 Å (8)
O9	−0.28	1	−3.81	−3.66	−3.40	−2.82	−1.75
O9.5	−0.27	1	−3.50	−3.45	−3.23	−2.78	−1.77
B0	−0.24	1	−3.20	−3.20	−3.00	−2.63	−1.68
B0.5	−0.22	2	−3.46 ± 0.04	−3.33 ± 0.02	−3.06 ± 0.13	−2.66 ± 0.07	−1.71 ± 0.06
B1	−0.19	3	−3.01 ± 0.08	−2.89 ± 0.06	−2.62 ± 0.04	−2.33 ± 0.03	−1.50 ± 0.02
B2	−0.17	1	−2.77	−2.64	−2.38	−2.14	−1.37
B3	−0.13	0	−2.45	−2.33	−2.04	−1.84	−1.21
B4	...	0	−2.15	−2.02	−1.73	−1.54	−1.05
B5	−0.09	2	−1.85 ± 0.11	−1.73 ± 0.11	−1.42 ± 0.02	−1.25 ± 0.07	−0.89 ± 0.06
B6	−0.07	1	−1.79	−1.64	−1.17	−1.02	−0.74
B7	−0.04	0	−1.70	−1.49	−1.05	−0.93	−0.64
B8	−0.02	1	−1.60	−1.42	−0.92	−0.85	−0.54
B9	+0.00	2	−0.47 ± 0.03	−0.58 ± 0.01	−0.40 ± 0.03	−0.28 ± 0.00	−0.44 ± 0.02
A0	+0.01	1	+0.45	+0.18	+0.32	+0.58	+0.22
A1	+0.03	0	+0.87	+0.44	+0.47	+0.73	+0.22
A2	+0.05	1	+1.24	+0.73	+0.60	+0.89	+0.23
A3	+0.06	0	+1.75	+1.05	+0.88	+1.13	+0.43
A4	+0.08	0	+2.27	+1.37	+1.16	+1.37	+0.63
A5	+0.10	1	+2.76	+1.64	+1.43	+1.59	+0.84
A6	+0.12	0	+3.33	+1.80	+1.52	+1.66	+0.88
A7	+0.13	0	+3.91	+1.95	+1.62	+1.74	+0.91
A8	+0.14	0	+4.47	+2.11	+1.73	+1.82	+0.94
A9	+0.14	0	+5.05	+2.26	+1.83	+1.90	+0.98
F0	+0.15	2	+5.63 ± 0.50	+2.39 ± 0.31	+1.89 ± 0.11	+1.98 ± 0.15	+1.02 ± 0.03
F1	+0.16	...	+6.00	+2.77	+2.27	+2.12	+0.84
F2	+0.18	...	+6.36	+3.14	+2.64	+2.26	+0.94
F3	...	...	+6.70	+3.76	+2.88	+2.44	+1.04
F4	...	...	+6.98	+4.40	+3.10	+2.66	+1.12
F5	+0.26	...	+7.28	+5.00	+3.34	+2.90	+1.20
F6	...	...	+7.52	+5.52	+3.58	+3.10	+1.30
F7	...	...	+7.76	+5.96	+3.80	+3.30	+1.37
F8	+0.55	...	+8.00	+6.36	+4.04	+3.54	+1.48
F9	...	...	+8.22	+6.74	+4.30	+3.74	+1.58
G0	+0.82	...	+8.40	+7.08	+4.52	+3.96	+1.67
G1	+0.85	...	+8.60	+7.40	+4.78	+4.20	+1.76
G2	+0.88	...	+8.80	+7.68	+5.02	+4.38	+1.84
G3	+0.92	...	+8.96	+7.90	+5.24	+4.60	+1.96
G4	...	...	+9.12	+8.10	+5.48	+4.82	+2.10
G5	+1.00	...	+9.28	+8.32	+5.72	+5.08	+2.24
G6	+1.04	...	+9.42	+8.50	+5.96	+5.34	+2.38
G7	+1.10	...	+9.56	+8.66	+6.22	+5.60	+2.54
G8	+1.14	...	+9.72	+8.82	+6.48	+5.90	+2.70
G9	+1.16	...	+9.86	+8.98	+6.80	+6.16	+2.90
K0	+1.35	...	+9.98	+9.12	+7.14	+6.42	+3.09
K1	+1.45	...	+10.10	+9.24	+7.48	+6.70	+3.26
K2	+1.50	...	+10.20	+9.38	+7.78	+6.92	+3.44
K3	+1.55	...	+10.30	+9.48	+8.08	+7.14	+3.64
K4	+1.58	...	+10.46	+9.58	+8.36	+7.32	+3.82
K5	+1.60	...	+10.56	+9.64	+8.54	+7.48	+4.00
K6	+1.63	...	+10.66	+9.70	+8.72	+7.60	+4.14
K7	+1.65	...	+10.76	+9.72	+8.92	+7.70	+4.24
K8	...	...	+10.82	+9.76	+9.04	+7.84	+4.36
K9	...	...	+10.88	+9.76	+9.22	+7.94	+4.46
M0	...	...	+10.92	+9.76	+9.34	+8.04	+4.53
M1	+1.79	...	+10.98	+9.78	+9.46	+8.12	+4.60
M2	+1.79	...	+11.00	+9.78	+9.56	+8.18	+4.64
M3	+1.79	...	+11.02*	+9.78*	+9.66*	+8.24*	+4.68*
M4	...	...	+11.04*	+9.78*	+9.76*	+8.30*	+4.72*

The 1 σ scatter among several stars is frequently larger, probably as a result of inconsistent spectral types, reddening errors, and slight residual instrumental nonlinearities for the brighter stars.

Since the spectral type coverage earlier than F1 is reasonably good, the intrinsic colors for these spectral subtypes are given as observed or by linear interpolation. For later spectral types, however, the coverage is coarse and the observational scatter is large. The intrinsic colors were therefore read off from smooth curves hand-drawn through the data points. The individual observations used in this interpolation are given in Appendix B. Column 3 is therefore left blank for stars later than F1. Asterisks in columns (4) through (8) indicate that the values were obtained by extrapolation from data in Appendix B.

Recently, Gilra (1979) found that the standard *ANS* instrumental nonlinearity corrections are inadequate for bright stars. His results suggest that the intrinsic colors given here for O and B stars may be too red. However, most of the standard stars are well below 80,000 counts s^{-1} in all channels. Furthermore, there are usually several stars of different brightnesses measured for each spectral type. Thus, the error is expected to be <0.03 mag for the 1550, 1800, and 2200 Å channels and <0.05 mag for the 2500 and 3300 Å channels. These errors are within the rms scatter reported in the tables. Wesselius *et al.* (1979) are studying the intrinsic colors of early-type stars and intend to incorporate Gilra's correction factors. Precise colors will eventually become available, but the present data are sufficiently accurate for the purposes of this study.

APPENDIX B

OBSERVED INTRINSIC COLORS OF LATE-TYPE STARS

In Appendix A, the intrinsic colors of stars later than F0 are based on values read from smooth curves. For the sake of completeness, the observed intrinsic colors of stars later than F0 used to construct those curves are given in Table 8. If only one star is available the error bar represents the standard deviation of several observations; if only one observation is available for that star, it is the standard deviation of six or more samples in that observation. For the G2 II stars, no error bar is given for the 1550 and 1800 Å channels, because one of the stars was not detected in these channels.

TABLE 8

OBSERVED ULTRAVIOLET INTRINSIC COLORS, $(m_\lambda - V)_0$, OF STARS LATER THAN F0

Sp Type (1)	Number of Stars (2)	1550 Å (3)	1800 Å (4)	2200 Å (5)	2500 Å (6)	3300 Å (7)
F2 IV, V	7	6.40 ± 0.11	2.42 ± 0.14	1.31 ± 0.10	1.60 ± 0.09	0.40 ± 0.05
F2 Ia, Ib	2	6.36 ± 0.17	3.12 ± 0.13	2.21 ± 0.01	2.27 ± 0.01	0.98 ± 0.00
F3 IV, V	3	6.97 ± 0.25	3.14 ± 0.28	1.62 ± 0.10	1.84 ± 0.13	0.45 ± 0.05
F3 III	1	6.69 ± 0.22	3.45 ± 0.02	1.93 ± 0.01	2.09 ± 0.01	0.57 ± 0.01
F5 IV, V	5	7.45 ± 0.23	3.42 ± 0.12	1.77 ± 0.08	2.00 ± 0.06	0.50 ± 0.06
F6 IV, V	5	8.41 ± 0.29	4.52 ± 0.07	2.11 ± 0.01	2.32 ± 0.01	0.45 ± 0.02
F7 IV, V	3	8.54 ± 0.28	5.18 ± 0.10	2.35 ± 0.02	2.57 ± 0.01	0.48 ± 0.01
F8 IV, V	4	8.68 ± 0.21	5.88 ± 0.21	2.80 ± 0.11	2.90 ± 0.07	0.55 ± 0.04
F8 Ia, Ib	2	9.48 ± 0.26	6.54 ± 0.06	4.02 ± 0.06	3.66 ± 0.06	1.49 ± 0.10
F9 V	1	9.14 ± 0.12	6.23 ± 0.03	2.56 ± 0.00	2.68 ± 0.00	0.51 ± 0.00
G0 IV, V	3	9.85 ± 0.36	6.73 ± 0.30	3.28 ± 0.34	3.26 ± 0.22	0.64 ± 0.10
G0 II	1	8.97 ± 0.34	6.98 ± 0.07	4.58 ± 0.01	4.07 ± 0.01	1.26 ± 0.00
G0 Ib	1	...	8.05 ± 0.14	5.20 ± 0.01	4.52 ± 0.01	1.67 ± 0.00
G2 IV, V	3	9.53 ± 0.45	7.27 ± 0.09	3.73 + 0.18	3.58 ± 0.11	0.80 ± 0.07
G2 II	2	8.46	6.77	4.94 ± 0.33	4.41 ± 0.32	1.67 ± 0.09
G2 Ib	1	9.61 ± 0.16	7.82 ± 0.03	5.30 ± 0.01	4.66 ± 0.01	1.78 ± 0.00
G3 V	1	9.43 ± 0.78	7.41 ± 0.16	4.57 ± 0.03	4.10 ± 0.02	0.94 ± 0.00
G3 Ib	1	8.77 ± 0.87	7.30 ± 0.20	5.24 ± 0.04	4.87 ± 0.04	2.06 ± 0.00
G4 II–III	1	...	8.83 ± 0.10	5.96 ± 0.01	5.03 ± 0.10	1.48 ± 0.00
G5 IV, V	2	10.13 ± 1.32	8.12 ± 0.15	4.93 ± 0.14	4.31 ± 0.09	0.98 ± 0.07
G5 III	6	9.25 ± 0.26	6.52 ± 0.49	4.61 ± 0.31	4.32 ± 0.17	1.49 ± 0.04
G6 V	1	9.63 ± 1.08	8.34 ± 0.20	4.98 ± 0.01	4.40 ± 0.01	0.96 ± 0.00
G7 III	2	11.88 ± 0.19	9.22 ± 0.55	6.73 ± 0.71	5.49 ± 0.36	1.60 ± 0.09
G8 II, III	8	10.56 ± 0.27	9.62 ± 0.14	7.24 ± 0.19	5.88 ± 0.09	1.78 ± 0.02
G8 Ib	1	8.82 ± 0.33	7.88 ± 0.20	6.33 ± 0.09	5.85 ± 0.04	2.72 ± 0.02
G9 III	1	8.72 ± 0.33	10.14 ± 0.62	8.01 ± 0.04	6.32 ± 0.02	1.94 ± 0.00
K0 V	1	8.69 ± 0.96	9.31 ± 0.44	6.28 ± 0.03	5.27 ± 0.05	1.35 ± 0.00
K0 III	4	11.20 ± 0.19	10.14 ± 0.34	7.95 ± 0.19	6.56 ± 0.08	2.11 ± 0.08
K1 IV	1	...	9.45 ± 0.67	8.26 ± 0.07	6.59 ± 0.04	1.99 ± 0.00
K1 III	3	9.92 ± 0.54	9.84 ± 0.20	7.69 ± 0.48	6.28 ± 0.28	2.03 ± 0.07
K1 Ib	1	9.37 ± 0.64	9.04 ± 0.35	7.44 ± 0.05	6.60 ± 0.04	3.27 ± 0.00
K2 III	2	10.92 ± 0.22	...	9.48 ± 0.04	7.79 ± 0.08	2.64 ± 0.01
K3 II, III	4	10.63 ± 0.05	10.19 ± 0.16	8.81 ± 0.26	7.74 ± 0.15	3.14 ± 0.19
K3 Ib	1	11.48 ± 0.68	10.01 ± 0.20	8.66 ± 0.02	7.39 ± 0.02	3.45 ± 0.00
K4 III	1	...	...	10.75 ± 0.37	9.57 ± 0.27	5.05 ± 0.01
K5 II, III	2	10.76 ± 0.76	10.68 ± 0.54	9.43 ± 0.24	8.44 ± 0.24	4.14 ± 0.01
K5 Ib	1	10.55 ± 0.08	9.73 ± 0.03	8.30 ± 0.02	7.28 ± 0.02	4.05 ± 0.00
M0 III	1	8.84 ± 0.66	10.14 ± 0.68	9.72 ± 0.34	8.65 ± 0.18	4.25 ± 0.01
M1 III	1	9.83 ± 0.15	9.47 ± 0.45	9.48 ± 0.26	8.56 ± 0.33	4.21 ± 0.01
M2 Iab	1	10.24 ± 0.15	9.32 ± 0.05	9.13 ± 0.03	7.40 ± 0.01	4.63 ± 0.00
M3 III	1	11.26 ± 1.22	10.67 ± 0.54	10.03 ± 0.16	8.84 ± 0.12	4.43 ± 0.02

REFERENCES

Aalders, J. W. G., van Duinen, R. J., Luinge, W., and Wildeman, K. J. 1975, *Space Science Instrumentation*, **1**, 343.
Arp, H. C., and Brueckel, F. 1973, *Ap. J.*, **179**, 445.
Baldwin, J. R., Danziger, I. J., Frogel, J. A., and Persson, S. E. 1973, *Ap. Letters*, **14**, 1.
Burstein, D., and McDonald, L. H. 1975, *A.J.*, **80**, 17.
Butler, D., Carbon, D., Kraft, R. P. 1976, *Ap. J.*, **210**, 120.
Carruthers, G. R., Heckathorn, H. M., and Opal, C. B. 1978, *Ap. J.*, **225**, 346.
Ciardullo, R. B., and Demarque, P. D. 1978, in *IAU Symposium 80, The HR Diagram*, ed. A. G. Davis Philip and D. S. Hayes (Dordrecht: Reidel), p. 345.
Code, A., and Welch, G. 1979, *Ap. J.*, **228**, 95.
Cohen, J. 1979, *Ap. J.*, **228**, 405.
Coleman, G. D., Wu, C.-C., and Weedman, D. W. 1980, *Ap. J., Suppl.*, in press.
de Boer, K. S., and van Albada, T. S. 1976, *Astr. Ap.*, **52**, 59.
de Boer, K. S., and Koornneef, J. 1975, University of Groningen, Department of Space Research, unpublished internal rept. ROG 75-63.
de Vaucouleurs, G., and de Vaucouleurs, A. 1972, *Mem. R.A.S.*, **77**, 1.
Emerson, D. T. 1974, *M.N.R.A.S.*, **169**, 607.
Faber, S. M. 1972, *Astr. Ap.*, **20**, 361.
Fitzgerald, M. P. 1970, *Astr. Ap.*, **4**, 234.
Ford, H. C., and Jacoby, G. H. 1978, *Ap. J.*, **219**, 437.
Gallagher, J. S., Faber, S. M., and Balick, B. 1975, *Ap. J.*, **202**, 7.
Gilra, D. P. 1979, unpublished internal rept. ROG 79–13.
Greenstein, J., and Sargent, A. I. 1974, *Ap. J. Suppl.*, **28**, 157.
Harris, W. E. 1976, *A.J.*, **81**, 1095.
Hills, J. G. 1971, *Astr. Ap.*, **12**, 1.
Hodge, P. W. 1973, *Ap. J.*, **182**, 671.
Johnson, H. M., and Hanna, M. M. 1972, *Ap. J.* (*Letters*), **174**, L71.
Joly, M. 1974, *Astr. Ap.*, **33**, 1977.
Kester, D. 1976, University of Groningen, Department of Space Research, unpublished internal rept. ROG 76-13.
Kron, G. E., and Mayall, N. U. 1960, *A.J.*, **65**, 581.
Lamb, D. Q., Van Horn, H. M. 1975, *Ap. J.*, **200**, 306.
Larson, R. B., and Tinsley, B. M. 1978, *Ap. J.*, **219**, 46.
Lasker, B. M. 1970, *A. J.*, **75**, 170.
Light, E. S., Danielson, R. E., and Schwarzschild, M. 1974, *Ap. J.*, **194**, 257.
McClure, R. D., and Racine, R. 1969, *A.J.*, **74**, 1000.
O'Connell, R. W. 1976, *Ap. J.*, **206**, 370.
Oemler, A., and Tinsley, B. M. 1979, *A.J.*, **84**, 985.
Oke, J. B., and Schild, R. E. 1970, *Ap. J.*, **161**, 1015.
Peck, M. 1980, *Ap. J.*, **238**, in press.
Pritchett, C. 1977, *Ap. J. Suppl.*, **35**, 397.
Racine, R. 1971, *Ap. J.*, **168**, 393.
Rose, W. K., and Tinsley, B. M. 1974, *Ap. J.*, **190**, 243.
Sandage, A. R. 1961, *The Hubble Atlas of Galaxies* (Washington: Carnegie Institution of Washington).
Sandage, A. R., Becklin, E., and Neugebauer, G. 1969, *Ap. J.*, **157**, 55.
Sargent, W. L. W. 1968, *Ap. J.*, **152**, 885.
Schmidt-Kaler, Th. 1965, *Landolt-Börnstein Numerical Data and Functional Relationships in Science and Technology, Group 6, Vol. 1, Astronomy and Astrophysics*, ed. H. H. Voigt (Berlin: Springer-Verlag), p. 298.
Searle, L., and Zinn, R. 1978, *Ap. J.*, **225**, 357.
Spinrad, H., and Taylor, B. J. 1971, *Ap. J. Suppl.*, **22**, 445.
Tinsley, B. M. 1971, *Astr. Ap.*, **15**, 403.
———. 1978, *Ap. J.*, **222**, 14.
Tinsley, B. M., and Gunn, J. R. 1976, *Ap. J.*, **206**, 525.
Turnrose, B. E. 1976, *Ap. J.*, **210**, 33.
van den Bergh, S. 1969, *Ap. J. Suppl.*, **19**, 145.
van Duinen, R. J., Wu, C.-C., and Kester D. 1976, University of Groningen, Department of Space Research, unpublished internal rept. ROG 76-4.
van Duinen, R. J., Aalders, J. W. G., Wesselius, P. R., Wildeman, K. J., Wu, C.-C., Luinge, W., and Snel, D. 1975, *Astr. Ap.*, **39**, 159.
Wesselius, P. R., van Duinen, R. J., Aalders, J. W. G., and Kester, D. 1979, *Astr. Ap.*, in press.
Wu, C.-C., Gilra, D. P., and van Duinen, R. J. 1980, *Ap. J.*, submitted.

S. M. FABER: Lick Observatory, University of California, Santa Cruz, CA 95064

J. S. GALLAGHER: University of Illinois Observatory, Urbana, IL 61801

M. PECK: 5445 N. Sheridan, Apartment 3311, Chicago, IL 60640

B. M. TINSLEY: Yale University Observatory, Box 2023 Yale Station, New Haven, CT 06520

C.-C. WU: Code 685, NASA Goddard Space Flight Center, Greenbelt, MD 20771